ISSN: 1648-6897 / eISSN: 1822-4199

VILNIUS TECH
Vilnius Gediminas Technical University

JOURNAL of ENVIRONMENTAL ENGINEERING & LANDSCAPE MANAGEMENT

2024
Volume 32
Issue 3
Pages 191–200
https://doi.org/10.3846/jeelm.2024.21831

CLINOPTILOLITE- AND GLAUCONITE-BASED SORBENTS FOR LEAD REMOVAL FROM NATURAL WATERS

Kateryna STEPOVA✉, Roman KONANETS

Department of Environmental Safety, Lviv State University of Life Safety, 35 Kleparivska str., Lviv, Ukraine

Highlights:

- heat treatment of clinoptilolite contributes to an increase in sorption capacity;
- heat treatment reduces glauconite sorption capacity, microwaving improves it;
- physical adsorption prevails in the adsorption of lead by the studied samples;
- in microwaved samples interaction of adsorbate with adsorbent is faster.

Article History:

- received 23 November 2023
- accepted 10 April 2024

Abstract. The aim of the research is to determine the effect of heat treatment and microwave irradiation on the sorption properties of a natural clinoptilolite and glauconite to Pb^{2+} ions. To improve the sorption capacity the samples were heat treated at 550 °C for 3 hours or microwaved at 790 W for 30 minutes. The XRD and XRF analysis present the content of investigated samples and prove the increase in the sorption capacity after treatment. After contact with Pb, its content in the natural clinoptilolite increased to 2.66%, and in the thermally treated – to 6.035%. The PbO content in natural glauconite increased to 3.9%, but after microwaving it reached 5.2% of the total sample weight. Heat treatment is useful for improving the sorption capacity of clinoptilolite, and microwave irradiation can significantly increase the adsorption capacity of glauconite.

Keywords: wastewater, water pollution, water cleaning technologies, lead, adsorption, isotherm fitting, adsorption kinetics.

✉Corresponding author. E-mail: ***katyastepova@gmail.com***

1. Introduction

Lead is recognized worldwide as a serious environmental health risk that can cause serious adverse health effects, particularly in young children. It can persist in the environment for long periods and accumulate in organisms, leading to bioaccumulation and biomagnification along the food chain. There is evidence that approximately 80–90% of the daily dose of lead is ingested through food (Sobhanardakani et al., 2018). Most lead accumulates in predatory fish (tuna, shark), seafood, especially bivalves. The cause of lead in food is water pollution, that is a significant environmental issue that threatens aquatic ecosystems and human health worldwide. Lead is potentially toxic pollutant released into water bodies from various sources, including industrial discharges, mining activities (Bosak et al., 2020; Bosak & Stokalyuk, 2022), and improper electronic waste disposal (Moossa et al., 2023). Nowadays, hostilities in Ukraine have become an additional source of potentially toxic elements' pollution in natural waters. Although access to research is currently complicated, especially on the left bank of the Dnieper river, where Russian occupation forces are stationed, and full monitoring is not possible, the experience of previous armed conflicts indicates that heavy metal contamination of natural waters is inevitable (Paukštys et al., 1998; Barker et al., 2021). According to the investigation of the impacts of the First World War on the environment made by Heiderscheidt (2018), the amount of lead and copper present in soil within some areas (probably those that had been bombed the most by artillery) was significantly high. In Gillies et al. (2007) it was noted that particulates ejected from artillery strikes containing high levels of lead (Pb) and copper (Cu), which may be attributed to artillery shells and gun barrels, cause the contamination of the soils with these metals. Explosive grenades were also considered a significant source of high concentrations of lead (Pb) (Weber et al., 2020).

To mitigate water pollution caused by potentially toxic elements, improved wastewater treatment is necessary. There are several technologies used for removing potentially toxic elements from various sources such as wastewater, industrial effluents, and contaminated soil (Pandey et al., 2023; Gomase et al., 2022; Kumar et al., 2023; Okoro et al., 2022). The most commonly employed technology is adsorption on activated carbon (Omidi et al., 2019),

zeolites (Liu et al., 2023), or metal-based materials (Sobhanardakani et al., 2016; Talebzadeh et al., 2016; Topare & Wadgaonkar, 2023; Zanin et al., 2017). Different conventional techniques are used for the removal of organic (Kim et al., 2023; Li et al., 2024; Pandey et al., 2024; Saruchi et al., 2023), inorganic (Gomase et al., 2022; Kumar et al., 2023; Okoro et al., 2022) and biological contaminants (Kim et al., 2023; Pandey et al., 2024) for making water drinkable. Due to their availability and cost, sorbents based on natural minerals are promising materials for use in wastewater and gas treatment systems. Their main advantages are low cost, eco-friendliness, biodegradability, and non-toxicity.

Clinoptilolite-based sorbents have been extensively studied in recent years. Lots of modification methods for enhancing the sorption properties of clinoptilolite were suggested. The results of numerous studies represent promising backgrounds for clinoptilolite application as an effective adsorbent for the sustainable capturing of potentially toxic elements from wastewater. The result of the work (Stylianou et al., 2007) indicates that zeolite is efficient for Pb-, Zn-, and Cu-containing solutions. The use of the MoS_2-clinoptilolite composite and clinoptilolite for removing Pb from the solution showed that the modified composite had higher adsorption capacity than the parent compounds (Pandey et al., 2020). Clinoptilolite and zeolite-geopolymer foams (CFs) can be applied as sorbents for toxic metal ions removal from aqueous solution and CFs with higher content of clinoptilolite phase exhibit higher removal efficiencies for the five toxic heavy metals (Liu et al., 2023).

Glauconite has been widely used as an ion exchanger. It is promoted by such factors as the granular structure of glauconite, which allows carrying out the process of ion exchange in dynamic conditions, as well as a significant increase in the exchange capacity of glauconite as a result of various pre-treatment methods.

A considerable number of works are devoted to the investigation of the sorption properties of glauconite, as a rule, each group of researchers obtained very interesting and ambiguous results (Franus et al., 2019, Martemianov et al., 2020; Franus & Bandura, 2014). Qualitative and quantitative regularities of the exchange capacity of ionite have been revealed, which varies within 26...50 mg-eq/100 g of glauconite. For minerals of the glauconite group, usually, there are simultaneous adsorption and exchange processes, and it is often challenging to differentiate between them.

The use of glauconite as a sorbent is reasonable because of its satisfactory operational properties. Glauconite does not release toxic impurities into the aqueous phase, has a low cost, and is suitable for modification with subsequent improvement of its sorption properties.

Despite a significant amount of previous research on the influence of various factors on the sorption properties of clinoptilolite and glauconite, the effect of microwave irradiation has been scarcely described. The aim of the present research is to determine the effect of heat treatment and microwave irradiation on the sorption properties of a natural zeolite and clay mineral in relation to one of the most dangerous drinking water pollutants – lead.

2. Materials and methods

2.1. Preparation of the samples

In this study, clinoptilolite from the Sokyrnytsia deposit (Figure 1), Zakarpattia region, Ukraine (48.46531765753879, 23.40295984518311) with the following characteristics: pH of the water extract – 7.75; bulk density – 947 kg/m^3, and glauconite: pH of aqueous extract – 8.6; bulk density – 1049,85 kg/m^3, were used to study the suitability for the extraction of lead from contaminated waters. The washed and weighed samples were dried at 80 °C to a constant weight. After sieving, a fraction of particles of 0.8–1.2 mm size was selected as the most suitable for investigating the sorption properties.

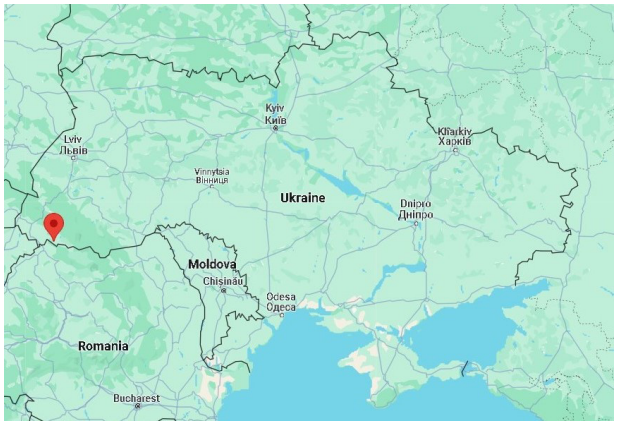

Figure 1. Capture of Sokyrnytsia deposit on the map

To improve the adsorption properties, the natural samples were exposed to heat treatment at 550 °C for 3 hours in a muffle chamber or to microwave irradiation for 30 minutes at 790 W.

2.2. XRD

X-ray diffraction experiments were performed using a standard powder diffraction procedure. XRD patterns were recorded on an AERIS Research (Malvern PANalytical) – CuKα, step size 0.022°.

XRF

XRF experiments were performed using Elvax Light SDD according to the requirements of ISO 29581.

PZC and pH effect determination

The isoelectric point of the materials was determined by the method reported in (Al-Maliky et al., 2021). 0.5 g of test sample was placed in 50 mL solution at different initial pH (1.0–13.0). In 24 h, the equilibrium pH of the solution was tested. Based on the plot of the dependence of the pH change on the initial pH value, the PZC was determined as the intersection of the plot with the x-axis.

2.3. Adsorption isotherms

Adsorption experiments were carried out using the batch method. Single-component model solutions were prepared from chemically pure $Pb(NO_3)_2$ anhydrous salt (Sfera Sim Ltd.). Eight jars (0.1 L) were filled with the appropriate solution, where 1 g of adsorbent was added, then stirred and left for 24 hours. The content of Pb^{2+} was determined by direct potentiometry (Ionometer AI-125). All experiments were repeated three times.

The correlation between the adsorbed amount of pollutant and its equilibrium concentration in solution was described by adsorption isotherms. In Table 1 theoretical models, that were chosen for non-linear fitting, are presented (Hu et al., 2023). The non-linear fitting was performed in GraphPad Prism 9.0 software.

Table 1. Isotherm models equations

Parameter No.	Isotherm model	Formula	Equation number
Two	Langmuir	$q_e = \frac{q_m K_L C_e}{1 + K_L C_e}$	(1)
	Fraundlich	$q_e = K_F C_e^{1/n}$	(2)
	Temkin	$q_e = \frac{RT}{b} \ln\left(K_T C_e\right)$	(3)
Three	Redlich-Peterson	$q_e = \frac{K_{RP} C_e}{1 + a_{RP} C_e^{\beta}}$	(4)
	Langmuir-Freundlich	$q_e = \frac{q_m \left(K_{LF} C_e\right)^{n_{LF}}}{1 + \left(K_{LF} C_e\right)^{n_{LF}}}$	(5)
	Hill	$q_e = \frac{q_H \times C_e^{n_H}}{K_D + C_e^{n_H}}$	(6)

2.4. Adsorption kinetics

Sorption kinetics is analyzed using well-known models: intraparticle distribution, Boyd, pseudo-first order (PFO), and pseudo-second order (PSO) models.

The intraparticle distribution model (Zhu et al., 2014) is presented by the equation:

$$q = k_{ip} \times t^{0.5} + C_i, \tag{7}$$

where k_{ip} is the rate constant, mg/g.min$^{0.5}$; C_i is the concentration at the level of the boundary layer i, mg/g. If $C_i < 0$, the control step is intraparticle diffusion; if $C_i > 0$, the adsorption process is quite complex and involves more than one diffusive stage.

Boyd model (Zhu et al., 2014) is supposed to be used for determination of rate-controling step and is expressed as follows:

$$F = 1 - \left(\frac{6}{\pi^2}\right) \exp\left(-B_t\right), \tag{8}$$

where B_t is the function of F, that is $F = q_t / q_e$, where q_t and q_e are the adsorbed matter at time t and at equilibrium state, respectively. In case $F > 0.85$, the B_t is expressed by equation:

$$B_t = -0.4977 - \ln\left(1 - F\right). \tag{9}$$

On the basis of $B_t = f(t)$ plot, the conclusion about the control factor is made.

The PFO model (Lagergren, 1898) is described by the following equation:

$$\frac{dq}{dt} = k_1\left(q_e - q\right), \tag{10}$$

where $q = q(t)$ is the concentration of the substance in the sorbent at time t; q_e is the equilibrium concentration in the sorbent, k_1 is the constant for the PFO model. The initial condition describing the absence of a substance in the sorbent at the initial time is $q(0) = 0$.

In the integrated form, the PFO model can be written as

$$q = q_e(1 - e^{-k_1 t}), \tag{11}$$

or reduced to a linearized form

$$\ln(q_e - q) = -k_1 t + \ln q_e. \tag{12}$$

The linearized Equation (12) is used to find the coefficient k_1 from the experimental data. This is done by plotting a trend line for the relationship between $\ln(q_e - q)$ and t. But this requires finding the equilibrium concentration in the sorbent q_e, which is often taken as the maximum concentration of a substance in the sorbent, or found by trial and error. Therefore, it is more expedient to use dependence (11) instead of (12), and to find the unknown parameters k_1 and q_e by finding a solution by minimizing the sum of the squared differences between the experimental and calculated values of the concentration of the substance q in the sorbent according to (11).

The PSO model (Ho & McKay, 1999) is also very often used to describe sorption kinetics. It is described by the equation:

$$\frac{dq}{dt} = k_2(q_e - q)^2, \tag{13}$$

where k_2 is the constant of the PSO model.

Taking into account the initial condition, in the integrated form the PSO model is as follows:

$$q = \frac{q_e^2 k_2 t}{1 + q_e k_2 t}, \tag{14}$$

or in the linearized form

$$\frac{t}{q} = \left(\frac{1}{q_e}\right) t + \frac{1}{k_2 q_e^2}. \tag{15}$$

In the case of the PSO model, unlike the PFO model, it's not difficult to find the values of the coefficients of

the linear relationship between t/q and t from the experimental data. Therefore, from the linearized Equation (15), we calculate q_e and k_2 from the experimental data, having previously found the coefficients of the trend line, and use them in the PSO model (13).

3. Results and discussion

3.1. Characterisation of the studied samples

X-ray diffraction patterns of natural clinoptilolite and glauconite are presented in Figure 2. The pattern indicates that the main phase in clinoptilolite is heulandite (04-011-6605 JCPDS card) with slight amounts of potassium aluminum silicon oxide hydrate (04-012-3686 JCPDS card), silicon oxide (00-061-0035 JCPDS card), and muscovite (01-082-0576 JCPDS card).

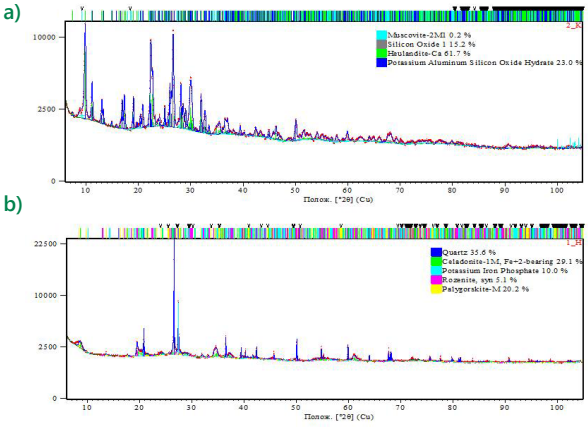

Figure 2. XRD pattern of a) natural clinoptilolite; b) natural glauconite

The heulandite and clinoptilolite have very similar X-ray diffraction patterns. The difference is in Si/Al ratio and Ca/K+Na content. In heulandite Si/Al < 4, and in clinoptilolite Si/Al > 4 (Bish & Boak, 2001). Na and K prevail in clinoptilolite, and Ca in heulandite (Ward & McKague, 1994). Considering the results of EDX analysis presented in Table 2, we may assume that the zeolite defined by the XRD pattern is clinoptilolite instead of heulandite.

Table 2. EDX of the natural clinoptilolite

Content, %								
O	Na	Mg	Al	Si	K	Ca	Ti	Fe
68.96	0.55	0.45	5.05	22.60	1.04	0.95	0.09	0.31

The pattern of the glauconite indicates that the main phases are quartz (01-070-3755 JCPDS card), celadonite (01-083-2008 JCPDS card) and palygorskite (04-018-3208 JCPDS card) with slight amounts of potassium iron phosphate (04-011-773 JCPDS card) and rozenite (04-015-4808 JCPDS card).

XRF

The results of the X-ray fluorescence analysis are presented in the Figures 3 and 4. It is obvious that the heat treatment of clinoptilolite significantly improves its adsorption capacity for lead, while it worsens it for glauconite. The initial PbO content in all the tested samples was < 0.01%, while after prolonged contact with Pb, its content in the natural clinoptilolite increased to 2.66%, and in the thermally treated sample to 6.035%. The microwave irradiation did not lead to significant changes in the sorption capacity of clinoptilolite, the PbO content increased only to 2.4%.

However, the sorption capacity of glauconite significantly improved under the influence of microwave irradiation. The PbO content in a sample of natural glauconite increased to 3.9%, but as a result of microwave irradiation, glauconite was able to absorb almost 1.5 times more PbO, and the content reached 5.2 % of the total sample weight. Thermal treatment reduces the sorption capacity of glauconite to 3.3% by weight.

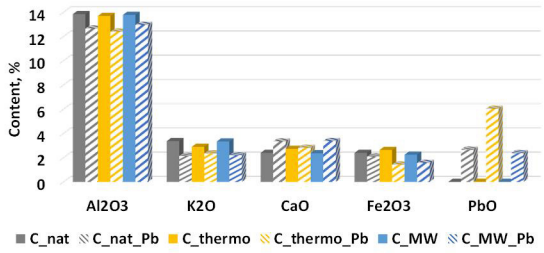

Figure 3. Results of XRF analysis of clinoptilolite samples before and after sorption

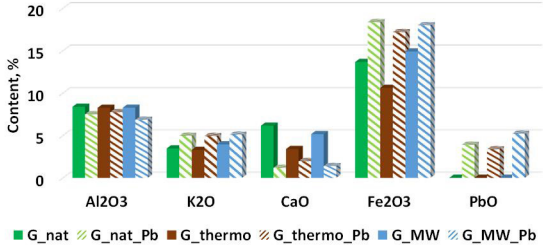

Figure 4. Results of XRF analysis of glauconite samples before and after sorption

PZC and pH effect determination

The Figure 5 shows the dependence of the pH change in the solutions upon contact with the test samples on the initial pH value. It is evident from the figure that the point of zero charge falls at a pH value of 7.5–8.

Since lead salts precipitate in an alkaline environment, the adsorption efficiency of the tested samples was determined in the pH range from 2 to 5.5.

The adsorption efficiency (a_{ef}) was determined according to the following equation:

$$a_{ef} = \frac{pH_i - pH_e}{pH_i} \times 100\%, \quad (16)$$

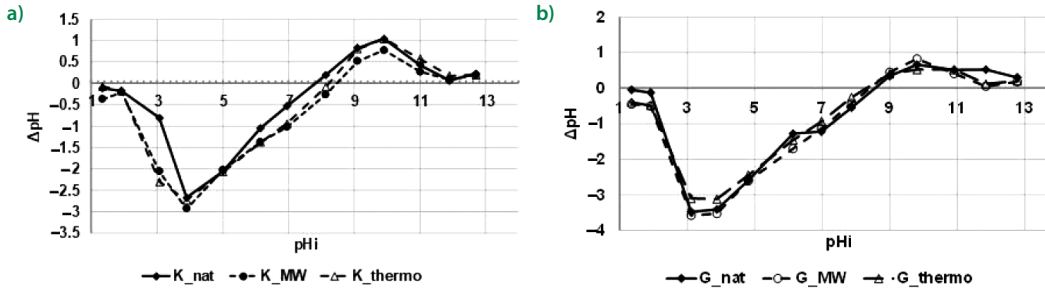

Figure 5. PZC determination diagram for: a) clinoptilolite samples; b) glauconite samples

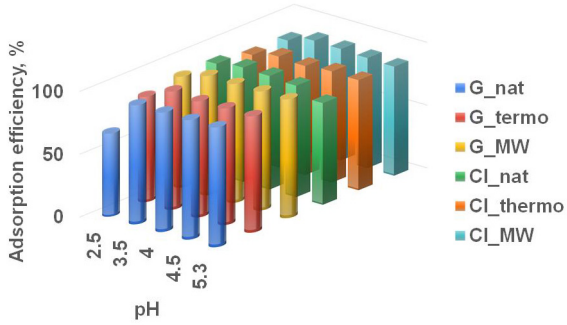

Figure 6. Diagram of dependence of adsorption efficiency on initial pH

where pH_i and pH_e are the initial and the equilibrium pH of the solution, respectively.

According to the Figure 6, the adsorption efficiency of the samples at pH 2 is the lowest. With an increase in pH, the adsorption ability of the samples gradually increases, but already at pH 5.3 it begins to decrease. This trend is observed for all glauconite samples. In clinoptilolite samples, a decrease in the adsorption efficiency is observed already at pH 4.5.

3.2. Adsorption isotherms

The results of non-linear fitting performed in GraphPad Prism 9.0 software are presented in Table 3. The adsorption isotherms based on the results of nonlinear fitting are shown in Figures 7 and 8. According to the IUPAC classification (Thommes et al., 2015), adsorption isotherms correspond to type IV (mesoporous materials).

Three two-parameter models and three three-parameter models were used for modelling. The Langmuir and Freundlich models are the most widely used. The Langmuir model assumes that adsorption occurs in a monomolecular layer on a homogeneous surface, while the Freundlich model assumes that adsorption occurs in a polymolecular layer on a heterogeneous surface. In our case, both models describe the process with the same accuracy. The advantage of the Temkin model is its ability to ignore extreme values of the function, and the constant β, which is positive for all samples, indicates that this process is exothermic (Figure 7).

It is obvious that the three-parameter models describe the process better, with the values of the coefficient of determination tending to unity. They are suitable for representing adsorption equilibrium over a wide range of concentrations. In some respects, they are universal, as they can follow either the Langmuir or Freundlich model for certain coefficient values.

Since the exponent β of the Redlich-Peterson model of all samples tends to unity, the entire model becomes close to the Langmuir model at low concentrations and, moreover, indicates that the surface of the samples is homogeneous. We reach a similar conclusion for the Hill model.

Hill's model suggests cooperative adsorption. In this study the value of n_H for all samples, except natural

Table 3. Results of isotherms' fitting

Index	Cl_nat	Cl_ thermo	Cl_MW	G_nat	G_ thermo	G_MW
	Langmuir					
q_m	0.8126	0.8859	0.7748	0.8350	0.7513	5.4227
k	0.6357	3.916	0.5733	315.027	233.29	5.3978
R^2	0.83	0.94	0.82	0.97	0.96	0.77
	Freundlich					
n	2.368	2.491	1.921	2.8586	5.3259	4.7978
K	0.3306	0.7061	0.274	2.9179	0.954	1.7137
R^2	0.89	0.94	0.78	0.87	0.95	0.70
	Temkin					
b	36.58	13.51	11.76	13.62	27.39	13.81
K_T	258.5	50.33	4.193	3116	16005	4348
R^2	0.76	0.94	0.90	0.98	0.97	0.96
	Langmuir-Freundlich					
q_m	371.7	1.308	0.543	0.7026	3.6651	0.8818
K	$6.097 \cdot 10^{-8}$	1.284	1.081	498.71	0.0091	356.24
n	0.4228	0.6596	1.942	1.8054	0.2243	1.2976
R^2	0.89	0.95	0.84	1.0	1.0	1.0
	Redlich-Peterson					
K_{RP}	0.7483	6.934	0.4476	282.03	1129	314,81
a_{RP}	1.5475	8.823	0.53	281.4	1285	303,9
β	0.5967	0.7578	1	0.952	0.8569	0,981
R^2	0.90	0.95	0.98	0.99	0.97	0,99
	Hill					
q_H	3304	1.308	0.5738	0.7759	1.197	0.9602
n_H	0.4224	0.6597	2.160	1.185	0.3280	0.9824
K_D	9993	0.8477	0.9255	0.00084	0.4024	0.0037
R^2	0.89	0.95	0.94	0.98	0.98	0.99

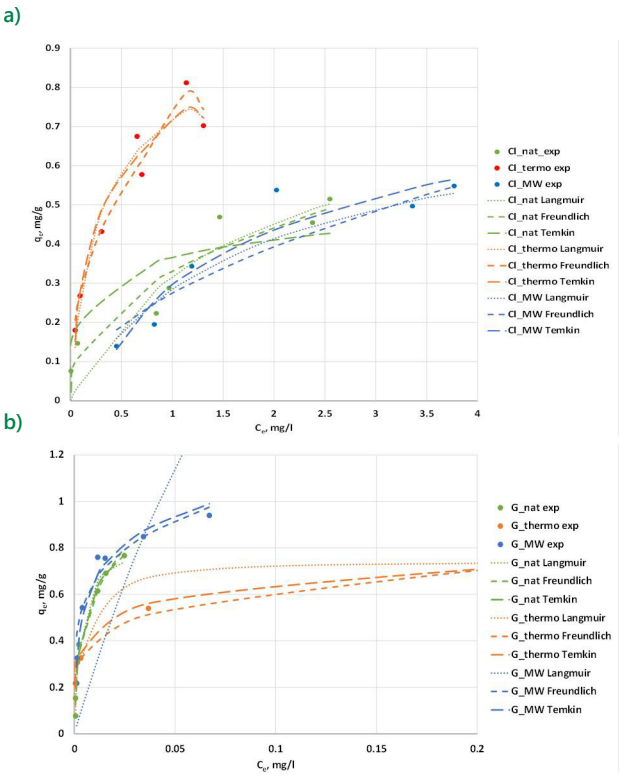

Figure 7. Two-parameter adsorption isotherms of Pb on a) clinoptilolite; b) glauconite

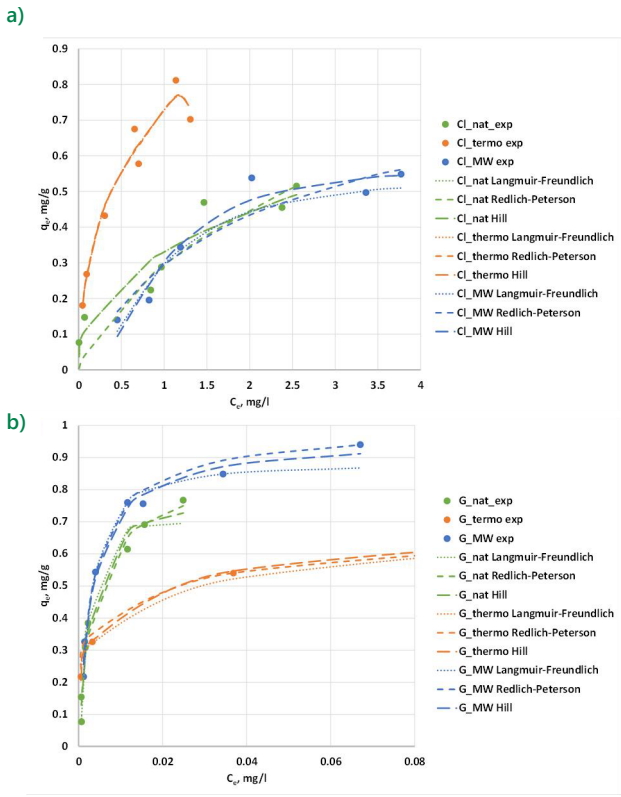

Figure 8. Three-parameter adsorption isotherms of Pb on a) clinoptilolite; b) glauconite

glauconite and microwaved clinoptilolite, is less than 1, so it corresponds to negative cooperativity in binding. High R^2 values and the n_H values also correspond to negative cooperativity in binding. The cooperative adsorption is consistent with the Langmuir isotherm observation (Figure 8).

As shown in Figures 7 and 8, heat treatment of natural clinoptilolite contributes to a significant increase in the sorption capacity, though it is not affected by microwave irradiation. On the contrary, thermal treatment of glauconite at 550 °C for 3 hours in a muffle chamber reduces its sorption capacity, instead of microwave treatment, which improves it. In Table 4 maximum sorption capacities of research samples (initial concentration of 500 mg/g) and similar adsorbents from another research are presented. The sorption capacity of the tested samples is comparable to the results reported by other researchers. The results correspond to adsorption isotherms in Figures 7 and 8. The highest adsorption capacities are inherent to microwave-treated glauconite and thermally-treated clinoptilolite. The calcination of clinoptilolite at 550 °C leads to an increase in the sorption capacity of the sample by 64%, while irradiation of glauconite with microwaves increases its sorption capacity by 15%. However, the sorption capacity of microwave-irradiated glauconite is higher than that of calcined clinoptilolite.

When the spent clinoptilolite samples in the amount of 5 g were kept for 48 hours in 100 ml of distilled water, the content of Pb^{2+} was below the detection limit of the device. Similar results were obtained in the case of glauconite test samples after sorption. Such results of the study of lead ion desorption from test samples fully coincide with the results obtained by Yanovska et al. (2008), Sabadash et al. (2017).

Table 4. Comparison of Pb^{2+} sorption capacities of different samples

Adsorbent	Maximum capacity, mg/g	Reference
NH_4-clinoptilolite, Ukraine	27.70	Sprynskyy et al. (2006)
Natural clinoptilolite, Mexico	32	Hernández-Montoya et al. (2013)
Natural clinoptilolite, Bulgaria	4.9	Panayotova and Velikov (2002)
Na-clinoptilolite, Italy	64.23	Cincotti et al. (2001)
Natural clinoptilolite, Croatia	84.59	Perić et al. (2004)
Natural clinoptilolite, Greece	44.86	Inglezakis et al. (2002)
Natural Egyptian glauconite (greensand)	21.654	Khaled et al. (2018)
Tunisian clay	27.15/ 40.75	Eloussaief and Benzina (2010)
Natural clinoptilolite (Ukraine)	25.5	This study
Heat treated clinoptilolite	41.18	This study

End of Table 4

Adsorbent	Maximum capacity, mg/g	Reference
Microwaved clinoptilolite	30.83	This study
Natural glauconite (Ukraine)	41.02	This study
Heat treated glauconite	31.14	This study
Microwaved glauconite	47.21	This study

3.3. Adsorption kinetics

The kinetic plots of lead sorption by natural, heat-treated, and microwave-treated glauconite for intraparticle distribution, Boyd, PFO, and PSO models are shown in Figures 9 and 10. The kinetic parameters determined from the examined models, as well as the R^2 determination coefficients, are shown in Table 5.

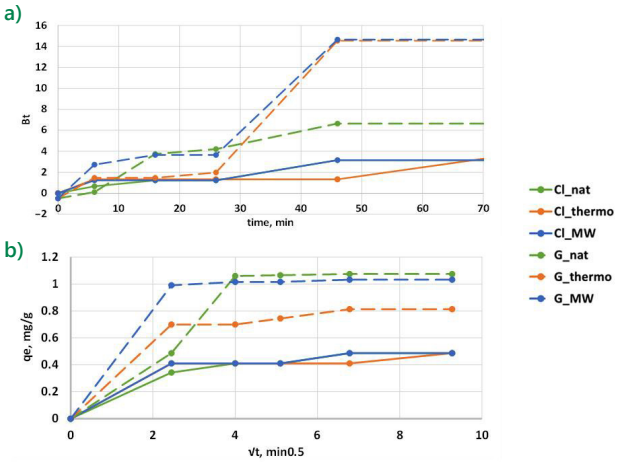

Figure 9. Pb^{2+} sorption kinetics models a) boyd; b) intraparticle distribution

As shown in Figure 9a the Boyd model plot of B_t versus t is nonlinear. As it was proposed in (Zhu et al., 2014), in such case the major dominating factor of the process may be either film-diffusion or external mass transport. From these plots it is possible to identify whether external transport or intraparticle diffusion controls the rate of adsorption. At the initial stage of adsorption process all plots were found to be linear, not passing through the origin. Moreover, the treatment of natural samples leads to a shift in the point of intersection of the line with the ordinate axis. This observation suggests that after treatment the participation of external mass transfer reduces giving a way to intraparticle diffusion control.

The intraparticle diffusion model for the adsorption of lead ions on the test samples is shown in Figure 9b. In (Zhu et al., 2014) it is stated that if the plot of q_e versus $t^{0.5}$ doesn't exhibit a straight line, the process is influenced by more than one step, so the intraparticle diffusion is not the only one limiting step. As presented in Figure 9, the plots of all test samples are presented by multilinear curves. Two linear areas were found on the graph, indicating that the adsorption of lead ions on the test samples is determined not only by intraparticle diffusion. It is possible that additional adsorption processes took place. Though the straight lines at the starting step went through the origin, indicating that the intraparticle diffusion is the rate-limiting step for initial stage od adsorption process. From the slope of the lines, it can be seen that the values of intercept, C, increased after treatment suggesting that surface adsorption became prominent. Such a trend would indicate that a higher amount of surface adsorption occur for treated samples than for natural ones, which lead to a reduction in the rate of diffusion of lead ions from the external surface of the sorbent to its internal surface. On the second step, it can be observed that the straight lines did not go through the origin, indicating that the factors of mass transfer will impact the adsorption process overtime.

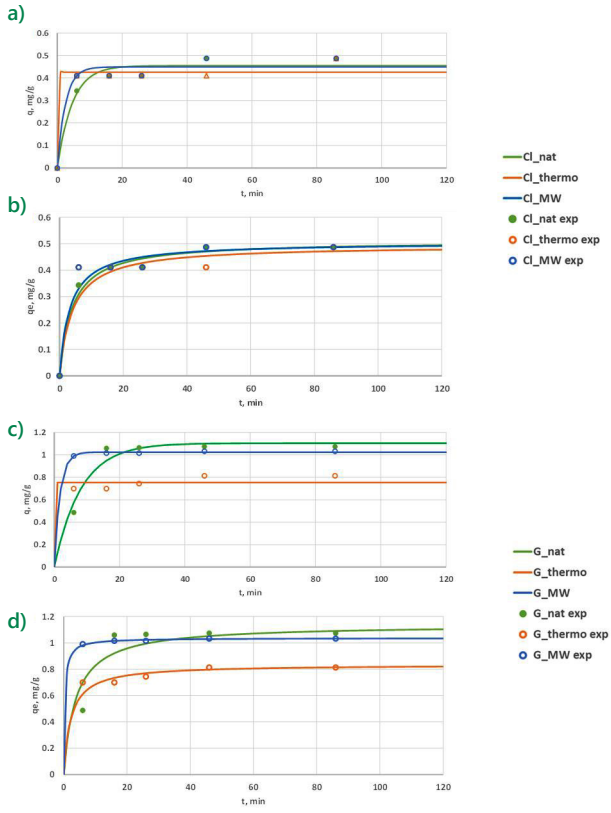

Figure 10. Pb^{2+} sorption kinetics models – Pseudo-First-Order: a) clinoptilolite samples, d) glauconite samples; Pseudo-Second-Order b) clinoptilolite samples, d) glauconite samples

The kinetic plots obtained using the pseudo-first and pseudo-second order models are shown in Figure 10. The kinetic parameters of Pb^{2+} adsorption determined from the graphs of the pseudo-first and pseudo-second order kinetic models are given in Table 5. It is evident that the sorption capacity of the heat-treated samples of both clinoptilolite and glauconite decreased. High values of the correlation coefficients of the pseudo-first-order model (R^2 = 0.97÷1) were obtained, which indicates that the process rate is controlled by adsorption processes. A weak interaction between the adsorbate and adsorbent surface controlled the adsorption process here. The adsorption

kinetics indicated that the calcined samples reach the adsorption equilibrium earlier in the first 5 minutes and their sorption capacity is the lowest. Microwave-treated samples reach the adsorption equilibrium a little earlier than natural samples, but their adsorption capacity does not decrease, which indicates a faster interaction of adsorbate with adsorbent.

Table 5. Parameters of the adsorption kinetics models

Index	Cl_nat	Cl_ thermo	Cl_MW	G_nat	G_ thermo	G_MW
	Pseudo-first order model					
q_e	0.455	0.426	0.449	1.104	0.754	1.024
k_1	0.217	60.0	0.40	0.123	60.0	0.571
R^2	0.97	0.97	0.97	0.98	0.97	1.0
	Pseudo-second order model					
q_e	0.510	0.494	0.505	1.138	0.835	1.036
k_2	0.503	0.499	0.625	0.234	0.543	2.855
R^2	0.94	0.46	0.76	0.82	0.89	1.0
	Intraparticle distribution model					
k	0.048	0.042	0.045	0.117	0.076	0.091
C	0.134	0.160	0.158	0.254	0.280	0.433
R^2	0.74	0.92	0.92	0.71	0.92	0.88

4. Conclusions

The effect of heat treatment and microwave irradiation on the Pb^{2+} sorption by a natural clinoptilolite and glauconite was investigated. The results of the X-ray fluorescence analysis proved that the heat treatment significantly improves the adsorption capacity of clinoptilolite for lead, but it worsens it for glauconite. While microwave irradiation slightly improves the sorption capacity of clinoptilolite, it significantly increases the adsorption ability of glauconite. The isotherm fitting showed that the adsorption process is consistent with the Langmuir isotherm, i.e., the process was characterized by the formation of a monolayer on a homogeneous surface. Kinetics modelling within the Boyd model suggests that after treatment the participation of external mass transfer reduces giving a way to intraparticle diffusion control. The intraparticle diffusion model indicate that the adsorption of lead ions on the test samples is determined not only by intraparticle diffusion. Though it is the rate-limiting step for initial stage of adsorption process. Higher amount of surface adsorption occurs for treated samples than for natural ones, which lead to a reduction in the diffusion rate of lead ions from the external surface of the sorbent to its internal surface. On the second step the factors of mass transfer will impact the adsorption process overtime. The adsorption kinetics indicated that the calcined samples reach the adsorption equilibrium most rapidly but this was followed by losses in adsorption capacity. Microwave treatment accelerates the interaction of adsorbate with adsorbent, while not reducing the adsorption capacity of the samples. The sorption capacity of the tested samples is comparable to the results reported by other researchers. Thus, heat treatment is useful for improving the sorption capacity of clinoptilolite, and microwave irradiation can significantly increase the adsorption capacity of glauconite. Therefore, it is worth investigating the effect of such treatments on the sorption capacity of natural minerals for other metals and hazardous substances.

Acknowledgements

The XRD research was performed on the equipment of the Scientific Equipment Collective Use Center "Laboratory of Advanced Technologies, Creation and Physico-Chemical Analysis of New Substances and Functional Materials", Lviv Polytechnic National University (https://lpnu.ua/ckkno).

Author contributions

Kateryna Stepova: conceptualization, methodology, formal analysis, investigation, writing original draft, writing-review and editing, visualization, supervision. Roman Konanets: methodology, formal analysis, investigation.

Disclosure statement

No potential conflict of interest was reported by the authors.

References

Al-Maliky, E. A., Gzar, H. A., & Al-Azawy, M. G. (2021). Determination of Point of Zero Charge (PZC) of concrete particles adsorbents. *IOP Conference Series: Materials Science and Engineering*, *1184*, Article 012004. https://doi.org/10.1088/1757-899X/1184/1/012004

Barker, A. J., Clausen, J. L., Douglas, T. A., Bednar, A. J., Griggs, C. S., & Martin, W. A. (2021). Environmental impact of metals resulting from military training activities: A review. *Chemosphere*, *265*, Article 129110. https://doi.org/10.1016/j.chemosphere.2020.129110

Bish, D. L., & Boak, J. M. (2001). Clinoptilolite-Heulandite nomenclature. *Reviews in Mineralogy and Geochemistry*, *45*(1), 207–216. https://doi.org/10.2138/rmg.2001.45.5

Bosak, P., & Stokalyuk, O. (2022). Modeling distribution of pollutants originating from coal waste dumps of the Novovolynsk mining area in the environment. *Bulletin of Lviv State University of Life Safety*, *26*, 5–13. https://doi.org/10.32447/20784643.26.2022.01

Bosak, P., Popovych, V., Stepova, K., & Dudyn, R. (2020). Environmental impact and toxicological properties of mine dumps of the Lviv-Volyn coal basin. *News of the Academy of Sciences of the Republic of Kazakhstan. Series of Geology and Technical Sciences*, *2*(440), 48–58. https://doi.org/10.32014/2020.2518-170X.30

Cincotti, A., Lai, N., Orrù, R., & Cao, G. (2001) Sardinian natural clinoptilolites for heavy metals and ammonium removal: Experimental and modeling. *Chemical Engineering Journal*, *84*(3), 275–282. https://doi.org/10.1016/S1385-8947(00)00286-2

Eloussaief, M., & Benzina, M. (2010). Efficiency of natural and acid-activated clays in the removal of Pb(II) from aqueous solutions.

Journal of Hazardous Materials, *178*(1–3), 753–757. https://doi.org/10.1016/j.jhazmat.2010.02.004

Franus, M., & Bandura, L. (2014). Sorption of heavy metal ions from aqueous solution by glauconite. *Fresenius Environmental Bulletin*, *23*(3), 825–839.

Franus, M., Bandura, L., & Madej, J. (2019). Mono and poly-cationic adsorption of heavy metals using natural glauconite. *Minerals*, *9*(8), Article 470. https://doi.org/10.3390/min9080470

Gillies, J. A., Kuhns, H., Engelbrecht, J. P., Uppapalli, S., Etyemezian, V., & Nikolich, G. (2007). Particulate emissions from U.S. Department of Defense artillery backblast testing. *Journal of the Air & Waste Management Association*, *57*(5), 551–560. https://doi.org/10.3155/1047-3289.57.5.551

Gomase, V., Jugade, R., Doondani, P., Saravanan, D., & Pandey, S. (2022). Sequential modifications of chitosan biopolymer for enhanced confiscation of Cr(VI). *Inorganic Chemistry Communications*, *145*, Article 110009. https://doi.org/10.1016/j.inoche.2022.110009

Heiderscheidt, D. (2018). The impact of world war one on the forests and soils of Europe. Ursidae: The Undergraduate Research *Journal at the University of Northern Colorado*, *7*(3), 1–16.

Hernández-Montoya, V., Pérez-Cruz, M. A., Mendoza-Castillo, D. I., Moreno-Virgen, M. R., & Bonilla-Petriciolet, A. (2013). Competitive adsorption of dyes and heavy metals on zeolitic structures. *Journal of Environmental Management*, *116*, 213–221. https://doi.org/10.1016/j.jenvman.2012.12.010

Ho, Y. S., & McKay, G. (1999). Pseudo-second order model for sorption processes. *Process Biochemistry*, *34*, 451–465. https://doi.org/10.1016/S0032-9592(98)00112-5

Hu, Q., Lan, R., He, L., Liu, H., & Pei, X. (2023). A critical review of adsorption isotherm models for aqueous contaminants: Curve characteristics, site energy distribution and common controversies. *Journal of Environmental Management*, *329*, Article 117104. https://doi.org/10.1016/j.jenvman.2022.117104

Inglezakis, V. J., Loizidou, M. D., & Grigoropoulou, H. P. (2002). Equilibrium and kinetic ion exchange studies of Pb^{2+}, Cr^{3+}, Fe^{3+} and Cu^{2+} on natural clinoptilolite. *Water Research*, *36*(11), 2784–2792. https://doi.org/10.1016/S0043-1354(01)00504-8

Khaled, A. S., Rasha, S. E.-T., & Merit, R. (2018). Utilization of surface modified phyllosilicate mineral for heavy metals removal from aqueous solutions. *Egyptian Journal of Petroleum*, *27*(3), 393–401. https://doi.org/10.1016/j.ejpe.2017.07.003

Kim, S., Son, N., Park, S.-M., Lee, C.-T., Pandey, S., & Kang, M. (2023). Facile fabrication of oxygen-defective ZnO nanoplates for enhanced photocatalytic degradation of methylene blue and in vitro antibacterial activity. *Catalysts*, *13*(3), Article 567. https://doi.org/10.3390/catal13030567

Kumar, N., Gusain, R., Pandey, S., & Ray, S. S. (2023). Hydrogel nanocomposite adsorbents and photocatalysts for sustainable water purification. Advanced Materials *Interfaces*, *10*(2), Article 2201375. https://doi.org/10.1002/admi.202201375

Lagergren, S. (1898). About the Theory of so-called adsorption of soluble substances. *Kungliga Svenska Vetenskapsakademiens Handlingar*, *24*, 1–39.

Li, Ch., Wang, Z., Liu, Y., Li, A., Li, Y., Ren, R., Song, Z., Wang, Y., Qi, F., Xu, B., Guan, X., Ikhlaq, A., & Ismailova, O. (2024). Effective control of DBPs formation and membrane fouling in catalytic ozonation membrane reactor for municipal wastewater reclamation. *Separation and Purification Technology*, *330*(Part C), Article 125492. https://doi.org/10.1016/j.seppur.2023.125492

Liu, Y., Zhao, S., Qiu, X., Meng, Y., Wang, H., Zhou, S., Qiao, Q., & Yan, C. (2023). Clinoptilolite based zeolite-geopolymer hybrid foams: Potential application as low-cost sorbents for heavy metals. *Journal of Environmental Management*, *330*, Article 117167. https://doi.org/10.1016/j.jenvman.2022.117167

Martemianov, D., Plotnikov, E., Rudmin, M., Tyabayev, A., Artamonov, A., & Kundu, P. (2020). Studying glauconite of the bakchar deposit (Western Siberia) as a prospective sorbent for heavy metals. *Journal of Environmental Science and Health, Part A*, *55*(11), 1359–1365. https://doi.org/10.1080/10934529.2020.1794686

Moossa, B., Qiblawey, H., Nasser, M. S., Al-Ghouti, M. A., & Benamor, A. (2023). Electronic waste considerations in the Middle East and North African (MENA) region: A review. *Environmental Technology & Innovation*, *29*, Article 102961. https://doi.org/10.1016/j.eti.2022.102961

Okoro, H. K., Alao, S. M., Pandey, S., Jimoh, I., Basheeru, K. A., Caliphs, Z., & Ngila, J. C. (2022). Recent potential application of rice husk as an eco-friendly adsorbent for removal of heavy metals. *Applied Water Science*, *12*, Article 259. https://doi.org/10.1007/s13201-022-01778-1

Omidi, A. H., Cheraghi, M., Lorestani, B., Sobhanardakani, S., & Jafari, A. (2019). Biochar obtained from cinnamon and cannabis as effective adsorbents for removal of lead ions from water. *Environmental Science and Pollution Research*, *26*, 27905–27914. https://doi.org/10.1007/s11356-019-05997-z

Panayotova, M., & Velikov, B. (2002). Kinetics of heavy metal ions removal by use of natural zeolite. *Journal of Environmental Science and Health, Part A*, *37*(2), 139–147. https://doi.org/10.1081/ese-120002578

Pandey, S., Fosso-Kankeu, E., Spiro, M. J., Waanders, F., Kumar, N., Ray, S. S., Kim, J., & Kang, M. (2020). Equilibrium, kinetic, and thermodynamic studies of lead ion adsorption from mine wastewater onto MoS2-clinoptilolite composite. *Materials Today Chemistry*, *18*, Article 100376. https://doi.org/10.1016/j.mtchem.2020.100376

Pandey, S., Kim, S., Kim, Y. S., Kumar, D., & Kang, M. (2024). Fabrication of next-generation multifunctional LBG-s-AgNPs@g-C3N4 NS hybrid nanostructures for environmental applications. *Environmental Research*, *240*(Part 1), Article 117540. https://doi.org/10.1016/j.envres.2023.117540

Pandey, S., Makhado, E., Kim, S., & Kang, M. (2023). Recent developments of polysaccharide based superabsorbent nanocomposite for organic dye contamination removal from wastewater — A review. *Environmental Research*, *217*, Article 114909. https://doi.org/10.1016/j.envres.2022.114909

Paukštys, B., Fonnum, F., Zeeb, B. A., & Reimer, K. J. (1998). *Environmental contamination and remediation practices at former and present military bases*. Springer. https://doi.org/10.1007/978-94-011-5304-1

Perić, J., Trgo, M., & Vukojević Medvidović, N. (2004). Removal of zinc, copper and lead by natural zeolite–a comparison of adsorption isotherms. *Water Research*, *38*(7), 1893–1899. https://doi.org/10.1016/j.watres.2003.12.035

Sabadash, V., Gumnitsky, Y., Mylyanyk, A., & Romaniuk, L. (2017). Simultaneous sorption of copper and chromium cations to wastewater treatment. *Scientific Bulletin of UNFU*, *27*(1), 129–132. https://doi.org/10.15421/40270129

Saruchi, Kumar, V., Bhatt, D., Pandey, S., & Ghfar, A. A. (2023). Synthesis and characterization of silver nanoparticle embedded cellulose–gelatin based hybrid hydrogel and its utilization in dye degradation. *RSC Advances*, *13*, 8409–8419. https://doi.org/10.1039/D2RA03885D

Sobhanardakani, S., Ahmadi, M., & Zandipak, R. (2016). Efficient removal of Cu(II) and Pb(II) heavy metal ions from water samples using 2,4-dinitrophenylhydrazine loaded sodium dodecyl sulfate-coated magnetite nanoparticles. *Journal of Water Supply: Research and Technology-Aqua*, *65*(4), 361–372. https://doi.org/10.2166/aqua.2016.100

Sobhanardakani, S., Tayebi, L., & Hosseini, S. V. (2018). Health risk assessment of arsenic and heavy metals (Cd, Cu, Co, Pb, and Sn) through consumption of caviar of *Acipenser persicus* from Southern Caspian Sea. *Environmental Science and Pollution Research*, *25*, 2664–2671. https://doi.org/10.1007/s11356-017-0705-8

Sprynskyy, M., Buszewski, B., Terzyk, A. P., & Namieśnik, J. (2006). Study of the selection mechanism of heavy metal (Pb^{2+}, Cu^{2+}, Ni^{2+}, and Cd^{2+}) adsorption on clinoptilolite. *Journal of Colloid and Interface Science*, *304*(1), 21–28. https://doi.org/10.1016/j.jcis.2006.07.068

Stylianou, M. A., Hadjiconstantinou, M. P., Inglezakis, V. J., Moustakas, K. G., & Loizidou, M. D. (2007). Use of natural clinoptilolite for the removal of lead, copper and zinc in fixed bed column. *Journal of Hazardous Materials*, *143*(1–2), 575–581. https://doi.org/10.1016/j.jhazmat.2006.09.096

Talebzadeh, F., Zandipak, R., & Sobhanardakani, S. (2016). CeO_2 nanoparticles supported on $CuFe_2O_4$ nanofibers as novel adsorbent for removal of Pb(II), Ni(II), and V(V) ions from petrochemical wastewater. *Desalination and Water Treatment*, *57*(58), 28363–28377. https://doi.org/10.1080/19443994.2016.1188733

Thommes, M., Kaneko, K., Neimark, A. V., Olivier, J. P., Rodriguez-Reinoso, F., Rouquerol, J., & Sing, K. S. (2015). Physisorption of gases, with special reference to the evaluation of surface area and pore size distribution (IUPAC Technical Report). *Pure and Applied Chemistry*, *87*, 1051–1069. https://doi.org/10.1515/pac-2014-1117

Topare, N. S., & Wadgaonkar, V. S. (2023). A review on application of low-cost adsorbents for heavy metals removal from wastewater. *Materials Today: Proceedings*, *77*, 8–18. https://doi.org/10.1016/j.matpr.2022.08.450

Ward, R. L., & McKague, H. L. (1994). Clinoptilolite and heulandite structural differences as revealed by multinuclear magnetic resonance spectroscopy. *Journal of Physical Chemistry*, *98*, 1232–1237. https://doi.org/10.1021/j100055a031

Weber, A. K., Bannon, D. I., Abraham, J. H., Seymour, R. B., Passman, P. H., Lilley, P. H., Parks, K. K., Braybrooke, G., Cook, N. D. & Belden, A. L. (2020). Reduction in lead exposures with lead-free ammunition in an advanced urban assault course. *Journal of Occupational and Environmental Hygiene*, *17*(11–12), 598–610. https://doi.org/10.1080/15459624.2020.1836375

Yanovska, E., Zatovskyi, I., & Slobodyanyk, M. (2008). Scientific fundamentals of a non-waste technology for post-treatment of industrial wastewater from mixtures of heavy metal ions. *Environment Ecology and Safety of Life Activity*, *5*, 50–54.

Zanin, E., Scapinello, J., de Oliveira, M., Rambo, C. L., Franscescon, F., Freitas, L., de Mello, J. M., Fiori, M. A., Oliveira, J. V., & Dal Magro, J. (2017). Removal of heavy metals from wastewater by adsorption. *Process Safety and Environmental Protection*, *105*, 194–200. https://doi.org/10.5772/intechopen.95841

Zhu, W., Liu, J., & Li, M. (2014). Fundamental studies of novel zwitterionic hybrid membranes: Kinetic model and mechanism insights into strontium removal. *The Scientific World Journal*, *2014*(1), Article 485820. https://doi.org/10.1155/2014/485820